Hybrid Physical and Data-Driven Approaches for Structural Health Monitoring and Digital Twins

Journal of LOW FREQUENCY NOISE, VIBRATION AND ACTIVE CONTROL

Journal of Low Frequency Noise, Vibration and Active Control
2026, Vol. 0(0) 1–24

DOI: 10.1177/14613484261421404
journals.sagepub.com/home/lfn
Sage

Machine learning–enhanced structural health monitoring of the steel–glass exedra under year-round environmental loading

Marianna Crognale[1], Cecilia Rinaldi[1], Jacopo Ciambella[1] and Vincenzo Gattulli[1]

Abstract

This paper presents a comprehensive approach to dynamic identification and environmental effect filtering for the Exedra Hall at the Capitoline Museums in Rome. Measurements collected continuously over 1 year were analyzed using the Stochastic Subspace Identification (SSI) method to extract the modal parameters. A k-means clustering algorithm was employed to identify and track the first three natural frequencies. To address temperature-induced frequency variations, a feedforward Artificial Neural Network (ANN) was trained on 8 months of frequency and temperature data, enabling the isolation and removal of temperature effects from the identified frequencies. The filtered frequencies were extrapolated and validated against the identified data for the entire observation period. To improve robustness, physical plausibility, and extrapolation capability under seasonal transitions, a physics-informed neural network (PINN) constrained by finite-element-derived thermomechanical priors was additionally introduced. Finally, a model updating of the Finite Element Model (FEM), has been carried out to describe the temperature effect. This work contributes to Structural Health Monitoring (SHM) practices by integrating advanced identification techniques, machine learning, and model-based simulations.

Keywords

structural dynamics, vibration monitoring, AOMA, ANN, PINN

Introduction

Continuous monitoring of natural frequencies in civil engineering structures provides a unique and cost-effective means for automated assessment of their condition. Vibration-based methods can gather real-time data that reflects the structural health of buildings and infrastructure. Extracting dynamic features from vibrating structures and inspecting their variations has become an engineering practice for automated structural performance assessment and early-stage damage detection. Structural damage can often be identified through modifications in the global dynamic behavior of the structure, Deraemaeker et al.[1] This approach enhances structures' safety and integrity and aids in timely intervention before minor issues become significant failures. Using advanced techniques such as Operational Modal Analysis (OMA), engineers can collect and analyze data that reflects a structure's natural frequencies and mode shapes, providing critical insights into its condition. This is particularly advantageous for large and complex structures, where traditional inspection methods may be impractical or too costly. Natural frequencies serve as sensitive indicators of structural performance; they can reveal changes in stiffness and mass that may indicate damage or degradation. As a key component for enabling the implementation of OMA into continuous SHM schemes, considerable research efforts have been made in recent years to develop Automated Operational Modal Analysis (AOMA) techniques. AOMA represents an advancement over traditional OMA analysis by incorporating automation to enhance efficiency and reduce the need for manual intervention, which can be time-consuming and prone to human error. Both are output-only techniques used

[1]Department of Structural and Geotechnical Engineering, Sapienza University of Rome, Rome, Italy

Corresponding author:
Marianna Crognale, Department of Structural and Geotechnical Engineering, Sapienza University of Rome, Via Eudossiana 18, Rome 00184, Italy.
Email: marianna.crognale@uniroma1.it

to identify the modal parameters of a structure using its response to ambient vibrations. However, AOMA introduces automated data processing and analysis techniques to streamline identification, incorporating algorithms to automate the processing of raw vibration data, including noise reduction, filtering, and modal parameter extraction. Automation allows for continuous monitoring and real-time updates of modal parameters, enhancing the effectiveness of SHM systems and improving the accuracy and reliability of modal parameter identification. These techniques specifically focus on automating time-domain-based Stochastic Subspace Identification (SSI) methods,[2] on automated interpretation of stabilization diagrams, and on assessing the consistency of the identified system poles across varying model orders.[3] Once clearly spurious/mathematical poles are removed, a specific clustering technique must be implemented to group the poles tagged as stable into subsets of similar modal features.[4]

However, the accuracy of frequency identification is significantly influenced by environmental parameters, particularly temperature variations.[1,5,6] These fluctuations can lead to erroneous interpretations of the structural state if not correctly accounted for. Therefore, effective strategies must be implemented to isolate and remove temperature effects from the identified frequency data. Research has consistently shown that temperature variations significantly affect the vibration properties of structures. In Luo et al.,[7] the authors discuss how temperature changes can alter natural frequencies and damping ratios, which are critical for accurate Structural Health Monitoring (SHM). This effect is particularly pronounced in civil engineering applications, where large structures are subjected to varying thermal conditions. It is demonstrated that temperature fluctuations can lead to substantial changes in the dynamic response of structures, impacting their reliability and safety assessments. These findings emphasize the need to incorporate temperature effects into frequency identification methodologies. Advanced modeling techniques have been developed to simulate the impact of temperature on structural dynamics. Kang et al.[8] present a model for simulating temperature effects in structural health monitoring, utilizing Machine Learning (ML) approaches to predict how temperature influences vibration properties. This innovative approach allows for more accurate structural integrity assessments under varying thermal conditions. This task becomes even more critical when dealing with culturally significant buildings that represent historical heritage. The structural health of historical monuments is essential to their functionality. Moreover, preserving such structures necessitates a meticulous approach to monitoring, ensuring that any assessment reflects the actual condition of the building without the confounding influence of environmental changes. Special attention has been devoted to developing robust methodologies to correct for the temperature effects. The integration and interpretation of various data types are essential for the effective use of SHM Systems for structural state assessment and damage detection.[9,10] Research indicates that temperature changes affect material properties and structural stiffness, thereby altering natural frequencies. For instance, studies have shown that temperature-induced modifications can lead to frequency shifts that mimic signs of potential damage.[11] As vibration testing technology and data storage methods have advanced, there has been an increase in comprehensive correlation studies examining the relationship between temperature and modal parameters of structures. These studies typically utilize long-term data from structural health monitoring (SHM) systems, focusing on natural frequencies. Mousavi and Gandomi[12] have removed seasonal patterns by the Variational Mode Decomposition (VMD) algorithm, using a structure's natural frequency and corresponding Johansen cointegration residuals to train a Recurrent Neural Network (RNN). Xia et al.[5] studied the variations in the modal properties based on the acceleration data recorded in 26 h, demonstrating that the structure's natural frequencies generally decrease when the temperature increases. However, variations in the frequencies are minimal. Li and Zhang et al.[13] discussed the temperature effect factors on the natural frequency, including variations of elastic modulus, deformations, structural internal force, and boundary conditions induced by temperature, and the effects of both uniform and non-uniform temperature distributions were investigated. Regni et al.[14] examined the influence of temperature variations and wind intensity on the fundamental frequencies and modal damping ratios of the UnivPM Faculty of Engineering Tower, a ten-level reinforced concrete building monitored with low-noise accelerometers, demonstrating that for masonry towers, the thermal expansion affects stiffness due to microcrack reclosure. At the same time, the increase of external forces leads to nonlinear effects. Ubertini et al.[15] proposed a correlation analysis to remove the effects of environmental changes, especially ambient temperature, from seasonal variations and daily fluctuations of the natural identified frequencies. Their principal findings reveal that the natural frequencies exhibit a nonlinear decrease with rising temperatures, a trend that can be filtered out using dynamic regression models. In Jiao et al.,[16] the authors investigated how temperature affects the static mechanical properties of concrete, revealing a strong negative correlation with temperature. Specifically, temperature influences damage identification in structures, as variations in elastic modulus are primarily responsible for changes in frequency. Research on the temperature effect on natural frequencies of different types of buildings has also been reported.[17–20] Ding[21] and Li[21] addressed the temperature variation problem of the measured modal frequency of the steel box girder of a suspension bridge. They studied the daily and seasonal correlations of the frequency and temperature in detail. They concluded that temperature was the key source of modal variability, and there was an overall decrease in modal frequency with temperature for all identified modes. In addition,

the vibration mode's daily average modal frequency had an obvious seasonal correlation with the daily average temperature. These results highlight the importance of understanding environmental influences for effective damage detection and assessing the initial health of structures. Therefore, it is essential to incorporate temperature data into structural health monitoring (SHM) frameworks to differentiate between environmental effects and potential damage indicators. Based on a comprehensive analysis of the literature concerning the temperature effects during dynamic identification, several methodologies can be employed, which can be categorized as: (i) statistical correlation methods, establishing statistical relationships between temperature variations and modal properties to identify normal operational ranges and detect anomalies; (ii) time series analysis, utilizing time series decomposition techniques for distinguishing seasonal patterns from structural responses and accurately identifying frequency shifts attributable to structural issues; (iii) machine learning algorithms able to enhance the ability to classify frequency changes based on environmental conditions, improving predictive maintenance strategies. Machine learning algorithms, particularly Artificial Neural Networks (ANNs), have emerged as powerful tools for enhancing the accuracy of modal parameter identification by mitigating the influence of environmental factors, such as temperature, on structural dynamics. These methods significantly improve over traditional statistical and time series approaches by effectively capturing complex, nonlinear relationships between environmental conditions and modal frequencies.[22] Zhou et al.[23] investigated the use of ANNs for simulating and predicting temperature-induced modal variability, demonstrating that ANNs can effectively map temperatures to frequencies. Ding et al. have also highlighted temperature-induced variations of measured modal frequencies in a long-span suspension bridge, emphasizing the impact of temperature on structural dynamics.[21] Gu et al.[24] have used artificial neural networks for damage detection in structures under varying temperature conditions using a two-step procedure: in the first one, a multilayer artificial neural network that uses temperature variables in addition to the frequencies as the inputs, is explored to identify patterns in frequencies of undamaged structures under varying temperature condition; in the second step a novelty index is used to quantify the discordancy between patterns in undamaged cases and candidate cases. Other studies[25–27] have demonstrated the efficiency of different ANN architectures, such as Backpropagation Neural Networks (BPNN) and Support Vector Regression (SVR), in modeling the complex relationship between modal frequencies and temperature, thereby enabling more accurate and reliable structural health monitoring and predictive maintenance.

This paper presents a methodology for automatically identifying the frequencies associated with the Marcus Aurelius Exedra in the Capitoline Museum of Rome, where a long-term monitoring system has been installed.[28] The Exedra at the Capitoline Museums, designed by architect Carlo Aymonino, is a significant architectural achievement that houses critical historical artifacts, including the equestrian statue of Marcus Aurelius. Given its cultural value, monitoring its structural integrity is crucial. The approach combines the continuous dynamic identification of the main modal parameters during a 1-year monitoring period with a clustering-based technique for continuous frequency tracking and filtering of temperature effects on natural frequencies using a feedforward artificial neural network (ANN). To enhance generalization capability and ensure physical consistency of the learned temperature–frequency relationship, a physics-informed neural network (PINN) formulation is subsequently introduced, embedding thermomechanical constraints derived from finite element analyses. The dynamic identification was addressed by employing Stochastic Subspace Identification, while the automated interpretation of the resulting stabilization diagrams was addressed using the K-means algorithm. Finally, to enhance the SHM insights and understanding, a validation was conducted via Finite Element Method (FEM) analysis.

Proposed methodology

Given that natural frequencies of civil structures and temperature information can be quickly obtained using current sensing technologies and data analysis methodologies, the proposed Automated Operational Modal Analysis developed in this paper comprises a multistep procedure. This procedure uses the data-driven technique for dynamic identification (SSI-COV) that allows for the identification of Exedra's dynamic properties using output-only data, a K-means clustering algorithm that is an unsupervised clustering method that aims to partition a dataset into k groups (clusters), where each observation belongs to the cluster with the closest mean (centroid), and finally data filtering with ANNs. The second part presents a physics-based modeling analysis, including the Finite Element Model (FEM) and subsequent model updating, highlighting their role in interpreting, validating, and prognosticating structural behavior. The Data-Driven Identification and Filtering (SSI, k-means, and ANN) is described in Section Data-Driven Identification and Filtering (SSI, k-means, and ANN), while the Physics-Based Modeling and Updating (FEM and model calibration) and model interpretation are reported in Section Physics-Based Modeling and Updating (FEM and model calibration). A critical discussion of the model assumptions, simplifications, and physics-informed enhancements is provided in Section Limitations, Simplifications and Physics-Informed Enhancement, which outlines the methodological limitations

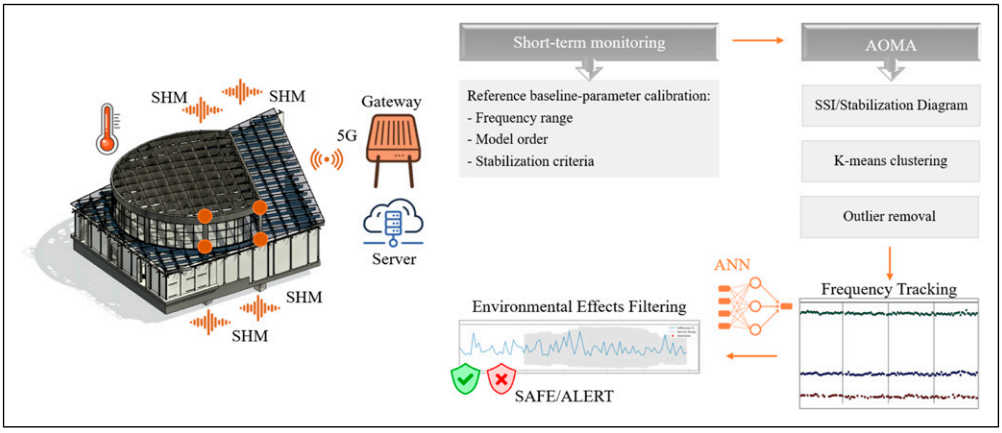

Figure 1. Workflow of the proposed study.

and potential extensions of the proposed framework. The overall procedure is illustrated in the accompanying diagram (Figure 1).

Data-driven identification and filtering (SSI, k-means, and ANN)

Automated long-term monitoring systems entail continuously collecting and analyzing sensor data over extended periods. This approach facilitates real-time assessments of system behavior without manual intervention. Key components of an automated monitoring framework include sensors for recording structural responses, centralized data storage for effectively managing large datasets, communication infrastructure for transmitting data from sensors to storage units, and processing units equipped with automated algorithms for real-time analysis. Vibration data were collected continuously for 1 year using triaxial MEMS accelerometers installed on the steel structure of Exedra Hall. The procedure adopted in this study to automate structural identification relies on identifying stable frequencies through a two-step method: the first step utilizes the SSI covariance-driven algorithm. This stage necessitates the prior definition of a reference baseline condition through short-term dynamic testing, which allows for the calibration of several parameters, such as the frequency range of interest, the model order, the stabilization criteria, the number of clusters (for the subsequent k-means processing step), and the threshold value (for outlier removal). The second step involves implementing k-means clustering, an unsupervised classification algorithm used to automatically group poles (eigenvalues) that correspond to the same physical mode. The k-means algorithm divides datasets into distinct clusters based on proximity to centroids derived from the data. It comprises three main steps: (i) initialization, where k initial centroids are randomly selected from the dataset; (ii) allocation, which assigns each data point to the nearest centroid's cluster; and (iii) centroid updating, which recalculates centroids based on the mean of all points assigned to each cluster. Assigning data points to the closest centroid and updating the centroids (steps 2 and 3) occur iteratively. This cycle continues until the convergence criteria are met, such as when the centroids do not change significantly between iterations or the assignments of data points to clusters remain unchanged. Once the automatic grouping process is complete, outliers are removed from the clustered groups, and the mean value is estimated. The mean value of the frequency is tracked over time by repeating the procedure for other datasets. A systematic approach that combines monitoring, data analysis, and interpretation is essential. The fluctuations in modal frequencies can be correlated with changes in environmental conditions such as temperature, humidity, wind, and pressure. These factors can significantly influence the behavior of the structure: temperature variations can cause expansion or contraction of materials, affecting the stiffness and consequently the modal frequencies; humidity may alter the mechanical properties of materials, leading to changes in the dynamic response[29]; rainfall can impact loads on the structure and the behavior of surrounding soil; wind action, mainly if intense and persistent, can induce forced vibrations in the structure, making more difficult the identification of natural frequencies, and the atmospheric pressure variations can indirectly affect measured modal frequencies through their coupling with air density.[30] In addition to these environmental factors, anthropogenic influences such as vehicular traffic, nearby construction activities, or even occupancy within the structure can introduce disturbances in the measurements and significant variations in mass, which can temporarily alter modal frequencies. It is crucial to correlate these factors with observed frequency variations over time, using filtering and analysis to identify recurring patterns or fluctuations attributable to environmental factors, thereby revealing reversible rather than permanent changes in structural health induced by damage or deterioration. Machine learning techniques can facilitate the development of predictive models that

account for multiple effects on modal parameters without the need to develop complex multi-physic models. By training models on historical data that includes temperature variations and corresponding frequency shifts, it is possible to predict future behavior under similar conditions. This predictive capability enhances the proactive management of structural health monitoring systems. To achieve this aim, the effect of temperature needs to be eliminated. ANNs (Goodfellow et al.[31] Haykin[32]) are computational models inspired by the functioning of the human brain. They consist of nodes (neurons) interconnected by weights, which are adapted during the training phase. In this context, ANNs are used to filter data, removing noise, anomalies, and artifacts, thus improving the quality of input data for subsequent models. ANNs are particularly effective in modeling complex nonlinear relationships. In this study, a feedforward ANN was designed to model the relationship between temperature variations and modal frequencies, as shown in Figure 2. Using 8 months of data for training and 4 months for validation, the network architecture consisted of (i) an Input layer: temperature data, (ii) Hidden layers, and (iii) an Output layer: residuals between raw and filtered frequencies. The trained model was applied to extrapolate filtered frequencies for the entire dataset. The performance was evaluated by comparing the ANN-filtered frequencies to the identified data.

Physics-based modeling and updating (FEM and model calibration)

To enhance the interpretation of the relationship between frequency and temperature, a detailed FE model was constructed based on Exedra's geometry, support conditions, and material properties (SAP2000). This analysis aims to understand the impact of temperature conditions on dynamic behavior, providing insights into structural interaction mechanisms.

Integrating Artificial Neural Networks (ANN) with physics-based FEM modeling significantly enhances conservation decision-making by the following:

(i) Providing environmentally robust data filtering: ANN effectively isolate and remove environmental effects (e.g., temperature fluctuations) from raw modal data, ensuring that identified frequency variations reflect genuine structural changes rather than environmental noise;
(ii) Enabling physically interpretable anomaly detection: The updated FEM incorporates refined boundary and interaction models informed by neural-network-filtered data, clarifying which variations stem from damage mechanisms versus natural or environmental factors;
(iii) Delivering a hybrid approach to risk assessment and intervention planning: The union of data-driven ANN insights with FEM predictive capabilities supports informed, adaptive maintenance strategies, minimizing false alarms and prioritizing interventions based on accurate, evidence-based structural health information;
(iv) Guaranteeing transferability and scalability: This hybrid framework can be adapted to other heritage structures with complex interactions, amplifying its utility in systematic preservation efforts.

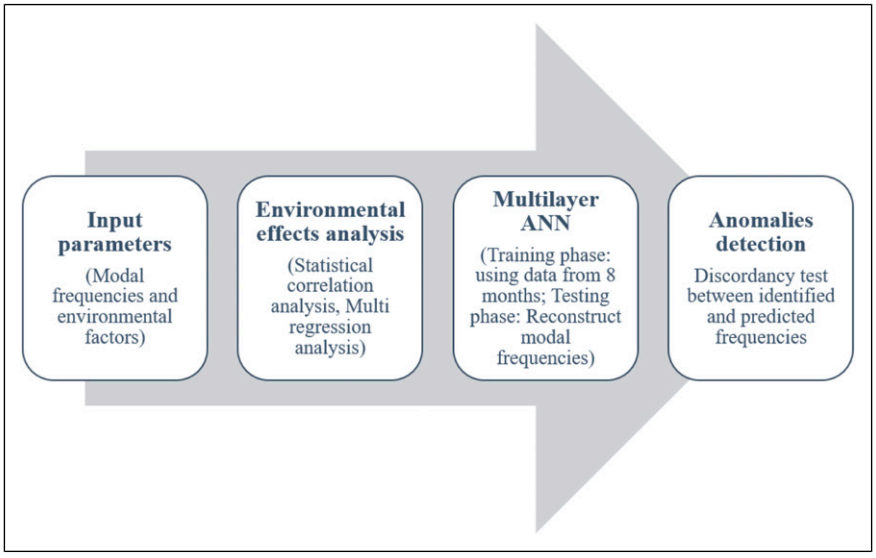

Figure 2. Schematic of the anomalies detection procedure.

The thermal analysis has been implemented on the FEM model of the structure, considering a uniform thermal load of ±25°C to evaluate stress changes due to seasonal temperature variations. For this purpose, the steel's material properties, including the coefficient of thermal expansion, have been first defined. This coefficient is crucial for assessing how the steel will expand or contract with temperature changes.[33] Subsequently, a model updating procedure was performed to represent the experimentally observed behavior of the Exedra structure analytically.

The continuous monitoring of the Marcus Aurelius Exedra

Data collection and AOMA

The described AOMA procedure has been exploited for the automated structural identification of the Marcus Aurelius Hall within Rome's Capitoline Museum complex. This structure features a semi-elliptical design supported by six steel columns that uphold massive girders holding glass enclosures (Figure 3(a). It is monitored through a system comprising a gateway and six wired sensor nodes (three on the roof and three on the lower level, as depicted in Figure 3(b) and (c) connected through Ethernet cabling designed to measure structural responses effectively. The installed SHM-Board is based on an ultra-low-power micro-controller capable of real-time SHM operations with high-performance interfaces connected to low-noise MEMS accelerometers. More in-depth explorations of the long-term monitoring system are described in Ref. [28]. A preliminary short-term acquisition phase provided reference data essential for establishing baseline parameters before implementing automatic processing algorithms. Integrating temperature variation data into Structural Health Monitoring can help better understand how environmental conditions affect the identified modal properties and distinguish between seasonal fluctuations in structural responses and those potentially indicative of structural damage. In addition to the existing vibration data, environmental parameters readings will be continuously acquired from the recording station of Roma Colosseo (LAT. 41.885297, LON. 12.495091) of the Institute for Atmospheric Sciences and Climate of the National Research Council (ISAC-CNR) web site, Meteo LazioTM amateur weather network (https://www.meteoregionelazio.it). The station is located a few hundred meters from the monitoring site, within the same urban canyon and topographic setting, and is therefore considered representative of the boundary environmental conditions acting on the Exedra structure. This data has been synchronized with vibration measurements to establish a comprehensive dataset. The operational modal analysis, which combines the k-means algorithm and the SSI procedure described in Section Data-Driven Identification and Filtering (SSI, k-means, and ANN), was implemented over a 1-year period from August 2023 to July 2024. Continuous tracking of the first three modal frequencies of the structure allows for identifying any variations over time.

The plots presented in Figure 4 illustrate the trends of the identified frequencies and temperature over the 12-month observation period for both daytime, 3:00 PM, Figure 4(a), and nighttime, 3:00 AM, Figure 4(b) periods. The identified frequencies for these time slots have been related to the maximum and minimum temperatures recorded. Preliminary

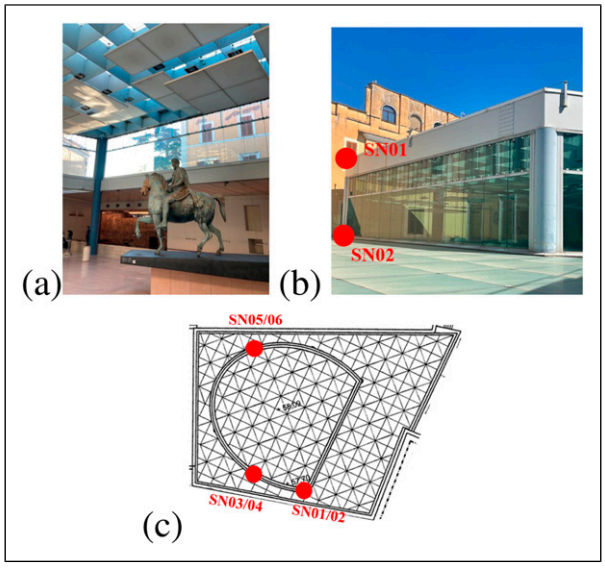

Figure 3. Marcus Aurelius hall in Capitoline Museum: internal view (a), external (b) and plan view (c) of the sensor layout.

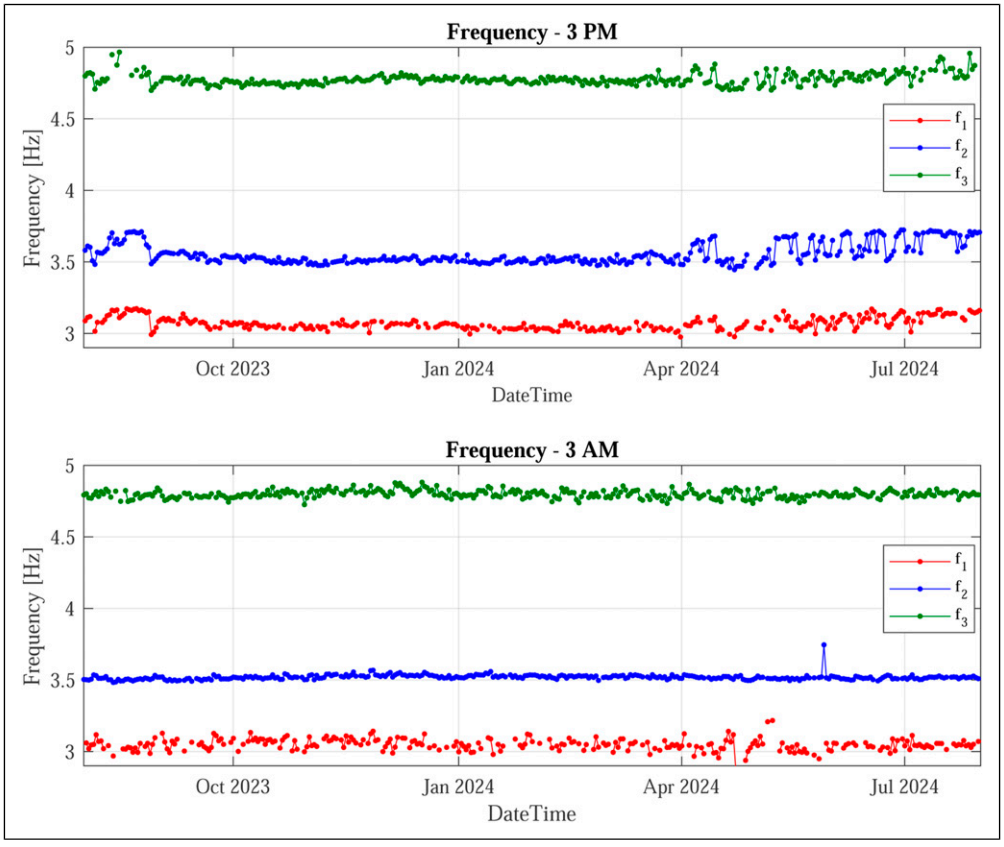

Figure 4. Frequency tracking (SN01) during August 2023 – July 2024 for daytime and nighttime.

observations suggest that frequencies exhibit greater variability during warmer months and are more pronounced during daytime hours. However, this alone is insufficient to indicate the presence of structural damage.

Environmental effect sensitivity analysis

Multiple Regression Analysis could be a suitable alternative to time series analysis for simultaneously exploring the relationships between several environmental parameter changes and dynamic frequency variations, and for identifying consistent patterns across seasons. It allows for modeling how temperature and relative humidity impact frequency changes more complexly and provides a fitting linear model. This means that each coefficient reflects the effect of that variable while controlling for the effects of the others. Multiple regression allows for the inclusion of multiple independent variables (predictors) to explain the variability in a single dependent variable (response). The general form of a multiple regression equation is expressed through the following equation (1):

$$y = \beta_0 + \beta_1 x_1 + \beta_2 x_2 + \epsilon \tag{1}$$

where y represents the dependent variable (dynamic frequency), x_1, x_2 are the independent variables (in this context, x_1 is for temperature, and x_2 is for relative humidity). β_0 is the intercept, which represents the expected value of y when all independent variables are zero. The partial regression coefficients β_1 and β_2 represent the partial effects of temperature and relative humidity on the frequency, respectively, while holding the other variable constant. A positive coefficient indicates that the dependent variable increases as the independent variable increases. A negative coefficient indicates that the dependent variable decreases in value. This is known as a partial effect. The term ϵ represents the error term or disturbance. It accounts for the variations in the dependent variable that are not explained by the independent variables included in the model. This error can arise from various sources, such as measurement errors, omitted variables, or random effects. The results of the multiple regression analysis, which considers all environmental factors simultaneously, are presented in Figure 5.

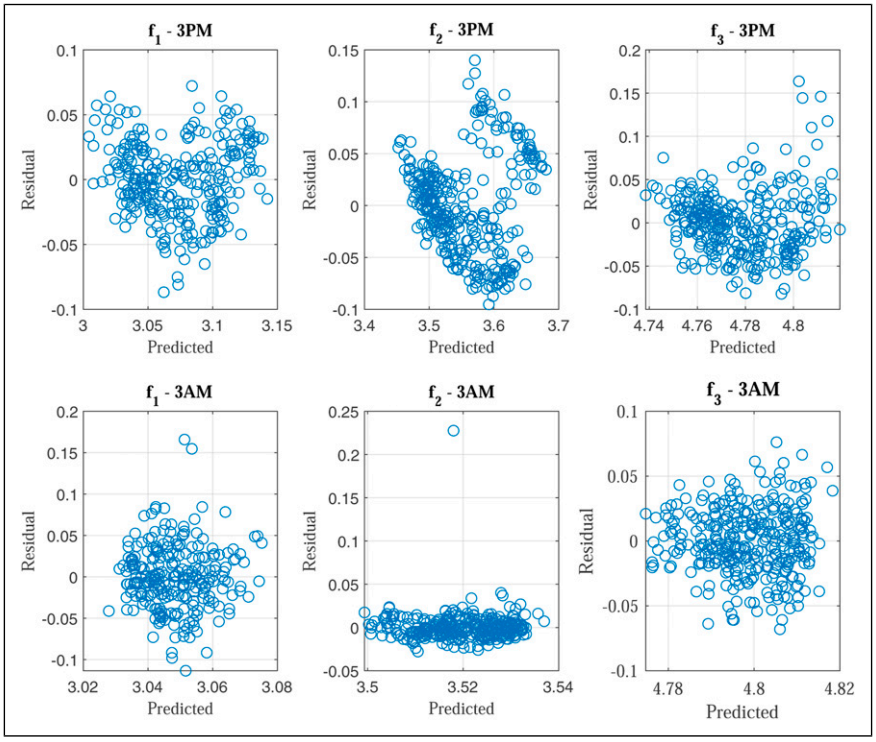

Figure 5. Plot of residuals versus predicted values via multiple regression analysis.

By observing the graphs, the residuals appear to be randomly distributed around zero, with no clear patterns for the first mode. During the day, the variance is likely to be slightly lower. Similar results could be observed for the third mode; the residuals appear randomly distributed around zero, but with more significant variance than the first mode. Some points deviate noticeably, suggesting less model accuracy. The second frequency exhibits a more considerable dispersion of residuals during the day, indicating lower accuracy of the model for specific predicted values. In contrast, during the night, the residuals appear concentrated near zero, with reasonably low variance, suggesting that the model isn't capturing all the data's variability. To validate the model's assumption, the Quantile-Quantile plot (Q-Q plot) were evaluated and reported in Figure 6 to verify the normality of the errors. If the residuals follow a normal distribution, points on the Q-Q plot should align closely with a straight diagonal line, with deviations indicating non-normality. The observed random scatter in residuals versus predicted values and points close to the diagonal line in the Q-Q plots strengthen confidence in the model. Table 1 summarizes the multiple regression parameters, revealing that temperature has a positive impact on frequency during the day and a negative effect at night, while relative humidity and pressure exhibit very weak and variable impacts on frequency (generally positive for pressure).

Given the dominant influence of temperature (with $|\beta_0|$ consistently larger than $|\beta_1|$, and recognizing that temperature is the most readily measurable and controllable environmental parameter in structural monitoring contexts, the subsequent analysis focuses specifically on the temperature–frequency relationship. To gain deeper insight into the temperature–frequency relationship, a dedicated correlation analysis was performed using the Pearson correlation coefficient. This analysis measures the strength and direction of the linear relationship between temperature and each natural frequency. The Pearson correlation coefficient r ranges from -1 to 1, where -1 indicates perfect negative correlation, 0 indicates no correlation, and 1 indicates perfect positive correlation.[34] Additionally, p-values were computed to assess statistical significance, with values less than 0.05 indicating that the correlation is unlikely to be due to random chance. The coefficient of determination R^2 was calculated to measure the proportion of variance in frequency explained by temperature variations. Figure 7 presents the linear regression results for the first three identified frequencies from both daytime (upper graphs) and nighttime (lower graphs) datasets. The blue dots denote experimental data points, while red lines represent linear interpolation curves. Additionally, Table 2 summarizes the coefficients obtained from linear regression and correlation analyses for the 6 data sets, related to the natural frequencies of three modes identified during the daytime and three modes identified during the nighttime. A striking positive correlation was found for daytime measurements, with strong correlation for the first two vibration modes (r = 0.7449 and 0.7572, respectively) and medium-strong positive correlation for the third mode (r = 0.4321). All p-values were less than 0.0001, confirming statistical significance. The coefficient of determination R^2 was

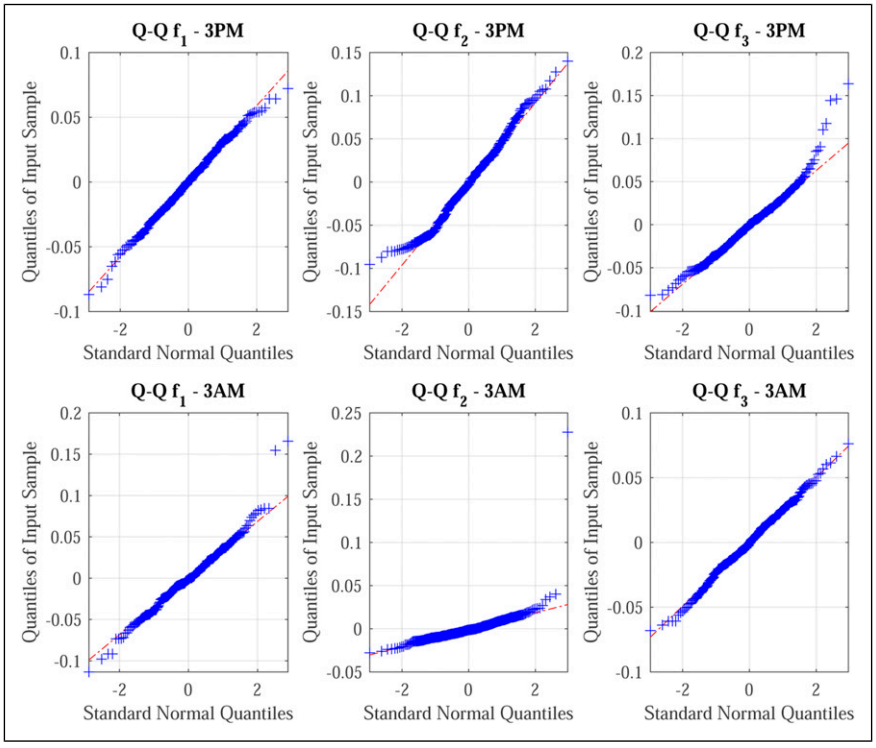

Figure 6. Quantile-Quantile plot.

approximately 0.56 for the first two modes, indicating that temperature explains about 56% of the variance in identified frequencies during daytime.

The nighttime datasets reveal weaker negative relationships with substantially less explanatory power. This diurnal variation in temperature sensitivity suggests complex thermomechanical interactions, potentially involving differential thermal expansion between the steel structure and the surrounding masonry, as well as variations in boundary conditions driven by thermal gradients. The positive correlation during daytime contradicts conventional expectations for steel structures, where thermal expansion typically reduces stiffness and consequently decreases natural frequencies. This anomalous behavior strongly suggests confinement effects from the surrounding historical masonry structure, as discussed in the subsequent finite-element analysis.

Neural network-based temperature filtering

Linear models in previous section captured the dominant temperature–frequency trend but leave structured residuals that indicate nonlinear and mode-dependent behavior. To obtain practically deployable filtering while retaining physical plausibility, we develop a neural filtering framework that combines a baseline feedforward Artificial Neural Network (ANN) with a Physics-Informed Neural Network (PINN). The baseline provides a transparent reference for achievable performance without physics guidance, whereas the PINN encodes thermomechanical priors derived from finite-element insights and

Table 1. Parameters of the multiple regression analysis.

	f(Hz)	β_0	β_1	β_2
Day	f_1	2.3306	0.0045	−0.0001
	f_2	3.0305	0.0072	−0.0005
	f_3	4.1495	0.0027	0.0001
Night	f_1	2.5788	−0.0014	−0.0000
	f_2	3.6294	−0.0013	0.0002
	f_3	4.7365	−0.0013	0.0004

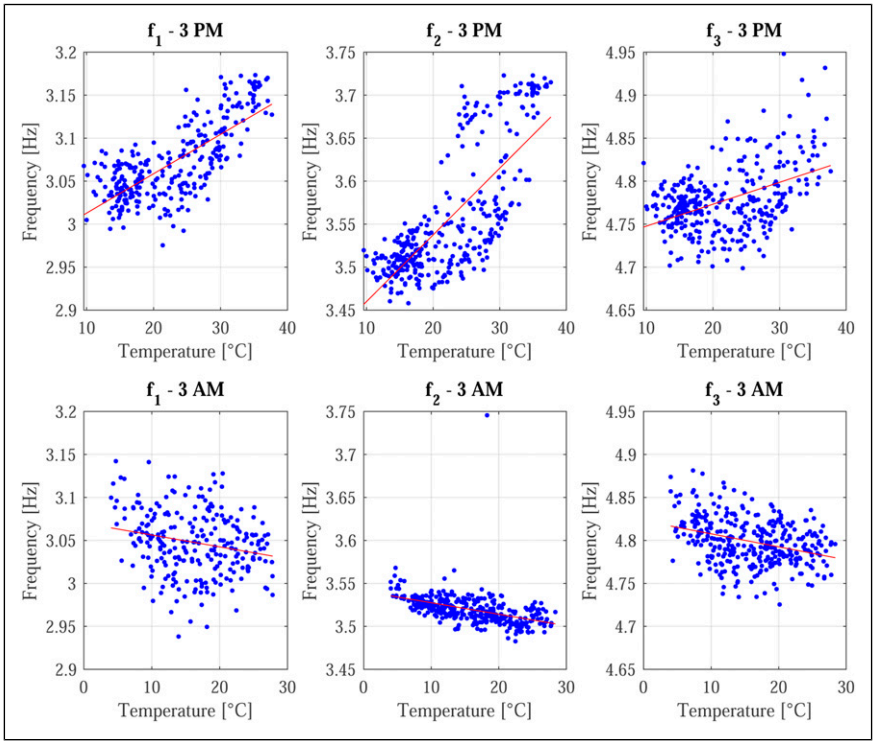

Figure 7. Frequency variation versus temperature for daytime in the upper row, and night time in the lower row, for the first three modes.

linear sensitivity analysis to improve generalization, robustness, and interpretability—requirements expected for Structural Health Monitoring (SHM) in heritage structures.

As baselines, we consider a feedforward ANN trained to map temperature to the identified frequency at each mode. The baseline is a 1–5–1 network with hyperbolic tangent activation, trained via trust-region reflective least squares (Scipy `least_squares` with finite-difference Jacobian); the network contains 16 parameters (5 input weights, 5 hidden biases, 5 output weights, 1 output bias), which facilitates convergence diagnostics and reduces variance. The training uses a strict temporal protocol: data up to 1 April 2024 are used for training and only subsequent observations are used for testing, preserving causality and avoiding information leakage that could inflate performance estimates in a monitoring setting.

For the first natural frequency (f_1), the ANN attains a test RMSE of 0.0628 Hz and a noise percentage decrease of 33.1%, indicating that temperature may not explain the fluctuations and suggesting unmodeled mechanisms (e.g., boundary condition variability). For f_2, performance is substantially better: the ANN reduces the standard deviation from 0.0517 Hz to 0.0357 Hz (30.3% noise reduction). For f_3, the improvement is modest (8.3% noise reduction), consistent with the weaker correlation with temperature (see Table 3). To further improve the capturing of unknown effects, a physics-based structure is added to the learning objective, especially for modes with weak linear temperature sensitivity or asymmetric day–night behavior.

To this end, we introduce a PINN with a dual-branch architecture that separates the dominant thermal response from residual, weakly nonlinear effects. A temperature main branch ($1 \to 32 \to 16 \to 1$ with `tanh`) captures the principal temperature dependence, while a lightweight residual branch (auxiliary features $\to 8 \to 1$ with `tanh`) models secondary influences such as seasonal encoding and temperature rate; the residual branch is L2-regularized with $\lambda = 10^{-4}$.

Table 2. Correlation coefficients of the linear relationship between frequencies and temperatures.

	f (Hz)	*r*-Pearson	*p*-value	R^2
T_{day} (°C)	f_1	0.7449	0.0000	0.5549
	f_2	0.7572	0.0000	0.5734
	f_3	0.4321	0.0000	0.1867
T_{night} (°C)	f_1	−0.2005	0.0013	0.0402
	f_2	−0.4454	0.0000	0.1984
	f_3	−0.3374	0.0000	0.1139

Table 3. Temperature filtering performance by mode. Noise reduction reported as percentage decrease in standard deviation (higher is better). Negative values indicate increased variance.

Mode	Lin. Regr.	ANN (LM 1–5–1)	PINN
f_1	31.4	33.1	33.8
f_2	28.7	30.3	33.0
f_3	4.2	8.3	8.3

Training minimizes a composite objective that balances data fit with physics priors:

$$\mathcal{L}_{\text{total}} = \mathcal{L}_{\text{data}} + \lambda_{\text{mono}}\mathcal{L}_{\text{mono}} + \mu_{\text{slope}}\mathcal{L}_{\text{slope}}.$$

The monotonicity term enforces sign-consistent temperature response in accordance with finite-element predictions of sensitivity from previous section:

$$\mathcal{L}_{\text{mono}} = \frac{1}{N-1}\sum_{i=1}^{N-1}\text{ReLU}\left(\text{sign}(\beta_{\text{FEM}})\cdot\frac{\Delta y_i}{\Delta t_i}\right)^2, \tag{2}$$

where samples are ordered by temperature and violations of the expected trend are penalized. The slope anchoring term ensures that the global temperature sensitivity matches the FEM-informed coefficient:

$$\mathcal{L}_{\text{slope}} = \left(\frac{\text{cov}(T,\widehat{f})}{\text{var}(T)} - \beta_{\text{FEM}}\right)^2. \tag{3}$$

Mode-specific regularization weights are selected by grid search over $\lambda \in \{0, 0.05, 0.1, 0.2, 0.5\}$ and $\mu \in \{0, 0.05, 0.1, 0.2, 0.5\}$. For f_1, we employ only the slope constraint $(\lambda_{\text{mono}}, \mu_{\text{slope}}) = (0, 0.05)$, which stabilizes the learned sensitivity without forcing strict monotonicity; for f_2 and f_3, the data are sufficiently self-consistent and the PINN reduces to the data term (0,0).

Filtering performance across methodologies is summarized in Table 3. The PINN achieves a slightly better variance attenuation on all modes, with marked gains on f_1 and f_3 where purely data-driven models underperform. Most importantly, the physics constraints provide guardrails against spurious extrapolation and yield estimates whose temperature sensitivities remain consistent with independent thermomechanical analysis, improving trustworthiness for SHM decision-making. The table reports Linear regression, the baseline ANN (LM 1–5–1), and the Physics-Informed NN.

Figures 8–10 present a comparative analysis of the original frequency measurements, the baseline ANN (LM 1–5–1), and the physics-informed neural network (PINN) estimates. Both neural network approaches effectively attenuate the seasonal variability in frequency, especially for f_1 and f_3. However, the PINN demonstrates superior performance in extrapolation, owing to its enforcement of monotonicity and slope constraints, which help preserve physical consistency outside the training domain.

To further contextualize these findings, Figure 11 presents the PINN filtering applied to all three modes together with temperature and the temporal train/test split. The physics-informed estimates preserve the dominant temperature-driven component while attenuating variability, most notably for f_1 and f_3.

The analysis clarifies the trade-offs between computational simplicity and physical fidelity. The compact baseline ANN trained via deterministic least-squares converges stably and is reproducible, but lacks guidance outside the training domain. In contrast, the physics-informed formulation demonstrates robust behavior during seasonal transitions (Figure 11), when purely data-driven models tend to degrade. By anchoring both the sign and the magnitude of temperature sensitivity through monotonicity and slope constraints, the PINN maintains physically plausible predictions even in sparsely sampled temperature ranges, thereby minimizing the physical frequency fluctuations with temperature.

Multi-method anomaly-detection framework for temperature-compensated structural health monitoring

Theoretical foundation and algorithmic architecture

Following temperature compensation via neural network filtering, a sophisticated anomaly-detection framework was implemented to identify potential structural irregularities in the filtered frequency domain. The proposed methodology

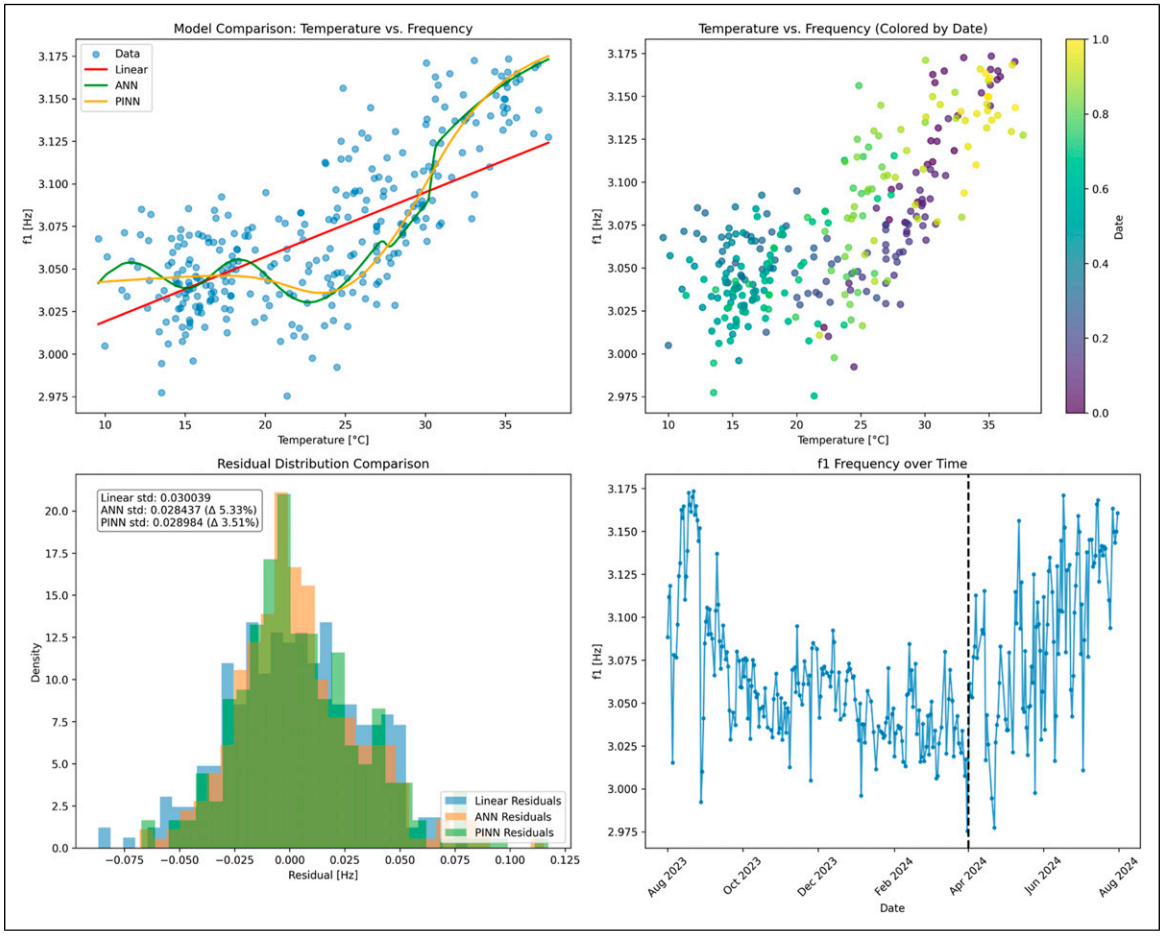

Figure 8. Comparative filtering for f_1: original frequency (blue), baseline ANN (LM 1–5–1, green), and physics-informed estimate (orange).

integrates a tripartite algorithmic architecture, wherein each component addresses distinct manifestations of anomalous behavior through complementary detection mechanisms.

Statistical Z-Score analysis. The primary detection mechanism employs standardized score analysis for global outlier identification. The deviation metric is formulated as

$$z_i = \frac{|f_i - \overline{f}|}{\sigma_f} \tag{4}$$

where f_i represents the filtered frequency at temporal index i, $\overline{f}$ denotes the empirical mean of the filtered frequency distribution, and σ_f represents the standard deviation. The detection criterion employs a threshold parameter $\tau = 3.0$, corresponding to a 99.73% confidence interval under Gaussian assumptions. This threshold selection represents an optimization between sensitivity to genuine structural anomalies and Type I error minimization, grounded in extreme value theory considerations.

Isolation forest IF algorithm. The secondary detection layer implements an unsupervised ensemble method predicated on isolation tree structures. The fundamental principle exploits the characteristic that anomalous observations require fewer random partitions for isolation compared to normal instances. The algorithm constructs $n_{\text{estimators}} = 100$ isolation trees, with each tree recursively partitioning the feature space through stochastic hyperplane selection.

The anomaly score for each observation is computed as

$$s(x, n) = 2^{-\frac{E[h(x)]}{c(n)}} \tag{5}$$

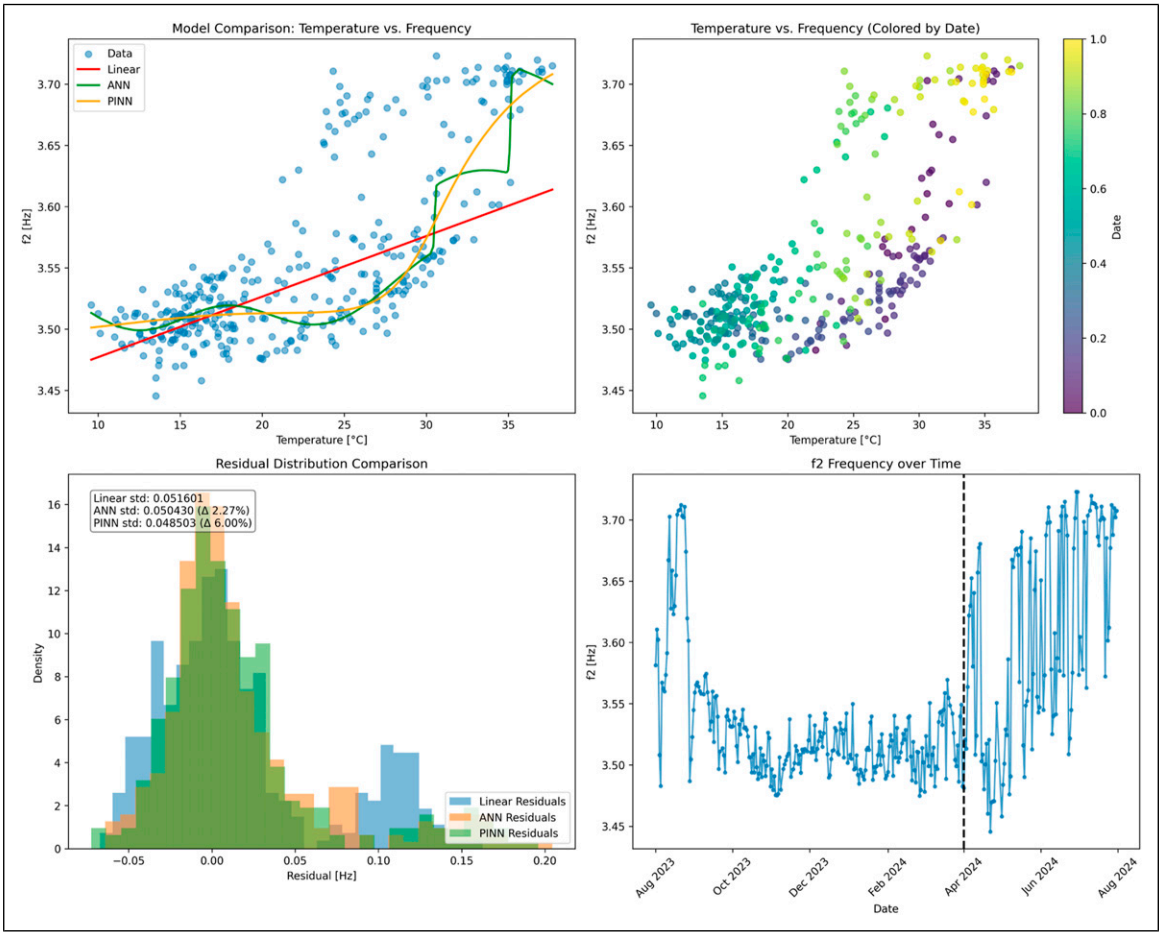

Figure 9. Comparative filtering for f_2: original frequency (blue), baseline ANN (LM 1–5–1, green), and physics-informed estimate (orange).

where $E[h(x)]$ represents the expected path length for instance x across all trees, and $c(n)$ denotes the average path length of unsuccessful searches in a Binary Search Tree structure. The contamination parameter $v = 0.05$ establishes the expected proportion of outliers within the dataset, directly influencing the decision threshold determination.

Local outlier factor analysis. The tertiary detection mechanism employs density-based anomaly identification through Local Outlier Factor (LOF) computation. This approach quantifies the local deviation of density for each observation relative to its k-nearest neighbors, where the neighborhood parameter is adaptively determined as

$$k = \min(20, \lfloor 0.5 n_{\text{test}} \rfloor) \tag{6}$$

This formulation ensures statistical stability while maintaining local sensitivity. The LOF score is formally expressed as

$$\text{LOF}_k(p) = \frac{1}{|N_k(p)|} \sum_{o \in N_k(p)} \frac{\text{lrd}_k(o)}{\text{lrd}_k(p)} \tag{7}$$

where $\text{lrd}_k(p)$ represents the local reachability density of point p, and $N_k(p)$ denotes its k-nearest neighborhood set. The detection threshold $\lambda_{\text{LOF}} = -0.8$ delineates anomalous instances based on empirically derived criteria specific to structural monitoring applications.

Temporal partitioning strategy

A critical methodological consideration involves the explicit exclusion of training data from anomaly detection procedures. This temporal partitioning strategy, implemented through the binary mask:

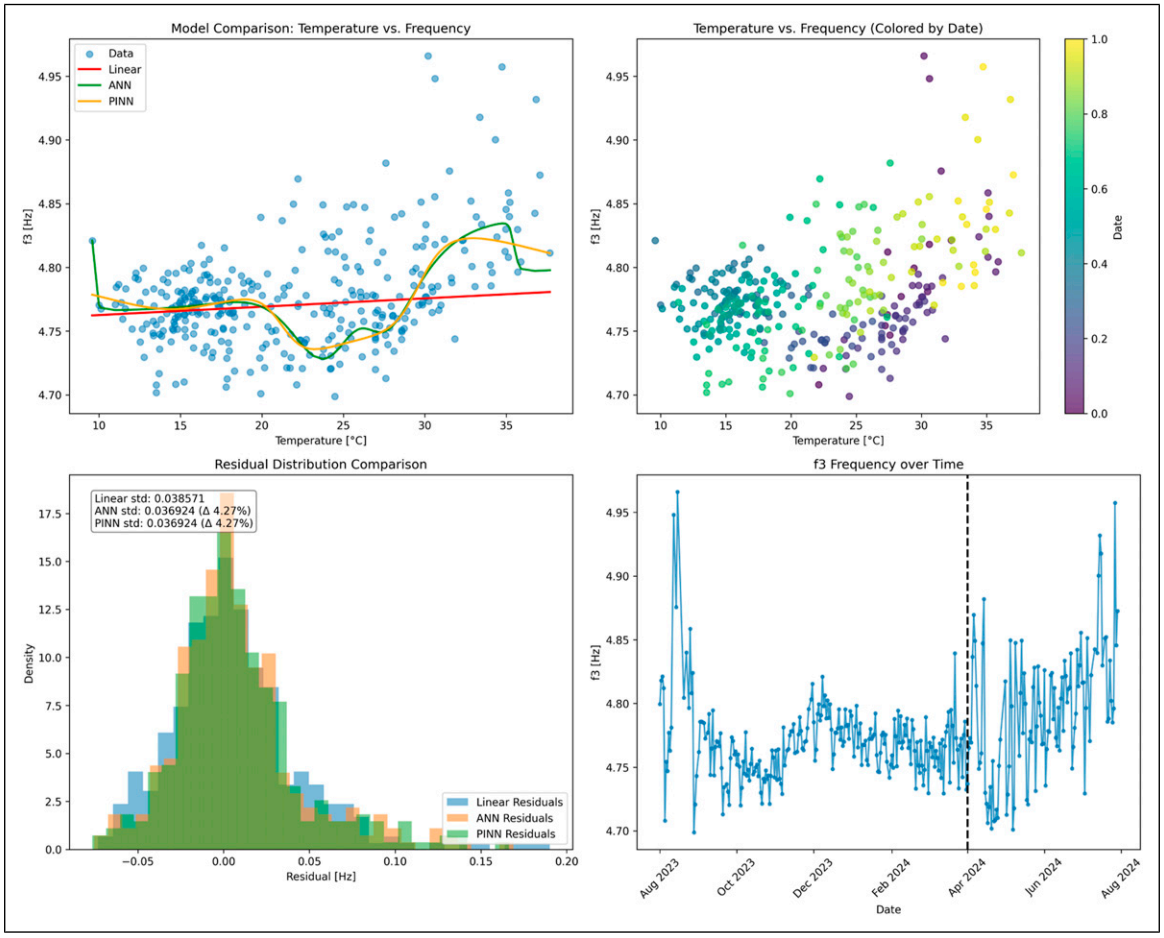

Figure 10. Comparative filtering for f_3: original frequency (blue), baseline ANN (LM 1–5–1, green), and physics-informed estimate (orange).

$$\mathcal{D}_{\text{test}} = \{i : t_i > t_{\text{cutoff}}\} \tag{8}$$

ensures that detection algorithms operate exclusively on the predictive domain (post-1 April 2024), thereby preventing overfitting artifacts and maintaining the integrity of the train-test separation paradigm. This approach preserves the causal structure of predictive modeling while ensuring that anomaly detection reflects genuine deviations in the operational phase rather than training artifacts.

Ensemble anomaly classification

The final anomaly classification employs a union operator across all detection methodologies:

$$\mathcal{A} = \{i \in \mathcal{D}_{\text{test}} : (z_i > \tau) \vee (\text{IF}_i = -1) \vee (\text{LOF}_i < \lambda_{\text{LOF}})\} \tag{9}$$

This inclusive approach maximizes sensitivity to diverse anomaly manifestations while leveraging the complementary strengths of each algorithm. The z-score method excels at identifying global statistical outliers, the Isolation Forest captures complex multivariate anomalies through ensemble partitioning, and the LOF algorithm detects local density deviations that might escape global detection schemes.

Parameter selection and optimization

The parameter selection reflects empirical optimization for structural health monitoring applications:

Figure 11. Combined physics-informed (PINN) filtering for f_1, f_2, and f_3 with temperature. The vertical dashed line marks the train/test split (1 April 2024).

1. **Z-score threshold** ($\tau = 3.0$): Corresponds to extreme value theory considerations, where exceedances beyond 3σ represent statistically significant deviations under normality assumptions.
2. **Contamination rate** ($\nu = 0.05$): Reflects domain expertise suggesting 5% anomaly prevalence in typical structural monitoring scenarios, balancing sensitivity against false positive rates.
3. **LOF threshold** ($\lambda_{\text{LOF}} = -0.8$): Empirically derived to optimize the trade-off between local sensitivity and false positive generation in time series contexts.

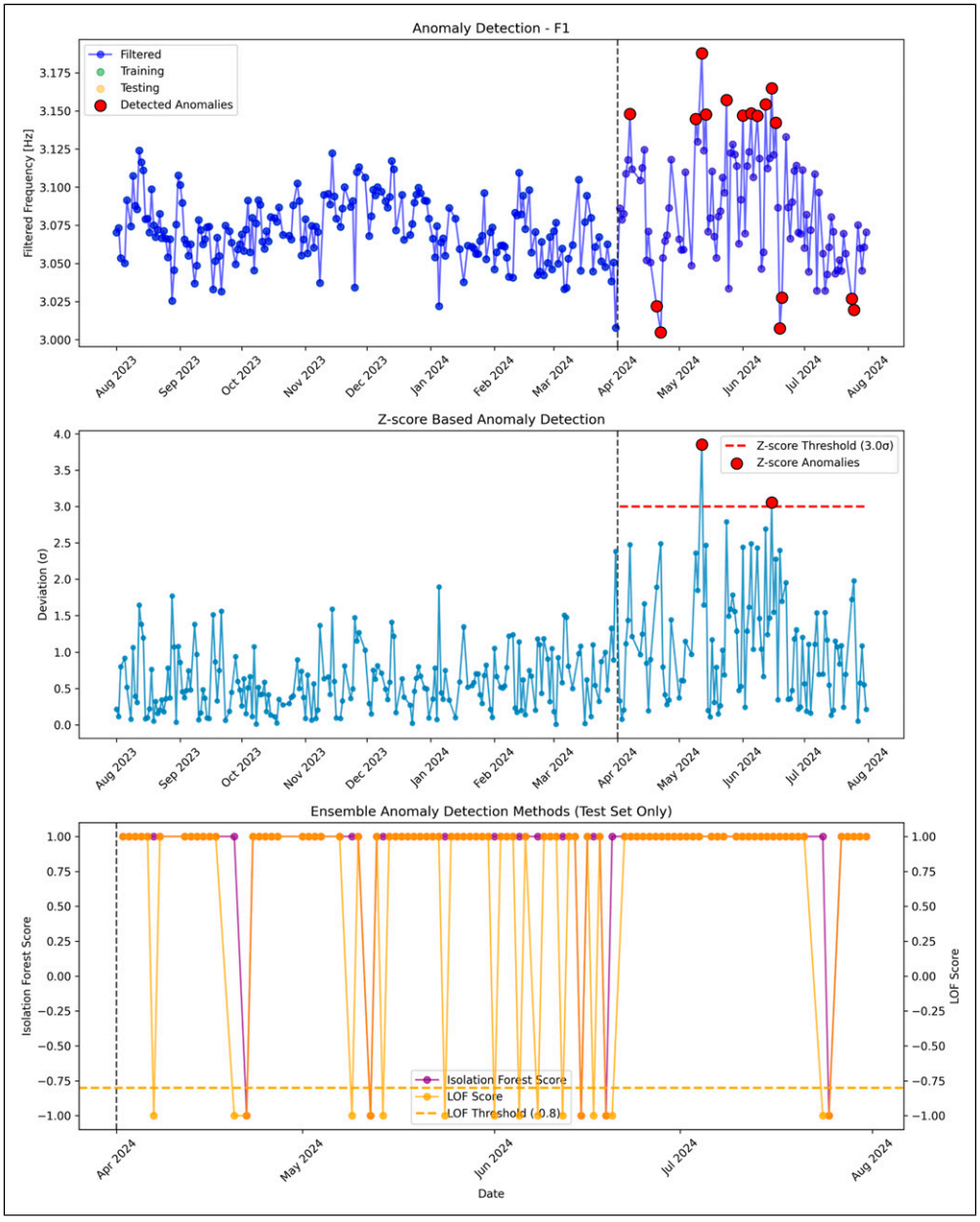

Figure 12. Multi-method anomaly detection results for the first natural frequency (f_1). The upper panel displays the filtered frequency with detected anomalies highlighted. The middle panel shows z-score deviations with the 3σ threshold. The lower panel presents the ensemble detection scores from Isolation Forest and Local Outlier Factor algorithms, demonstrating the complementary nature of the detection methodologies.

Anomaly detection results

Application of the multi-method framework to the temperature-compensated frequencies yielded the following detection statistics for the prediction period. Figures 12–14 present the comprehensive anomaly detection results for all three natural frequencies.

The temporal distribution of detected anomalies exhibited pronounced clustering during periods of rapid temperature variation, particularly in late spring and early summer transitions. This pattern suggests residual environmental coupling not fully captured by the temperature compensation models, potentially attributable to differential thermal expansion dynamics between the steel structure and confining masonry, or higher-order environmental interactions beyond univariate temperature effects.

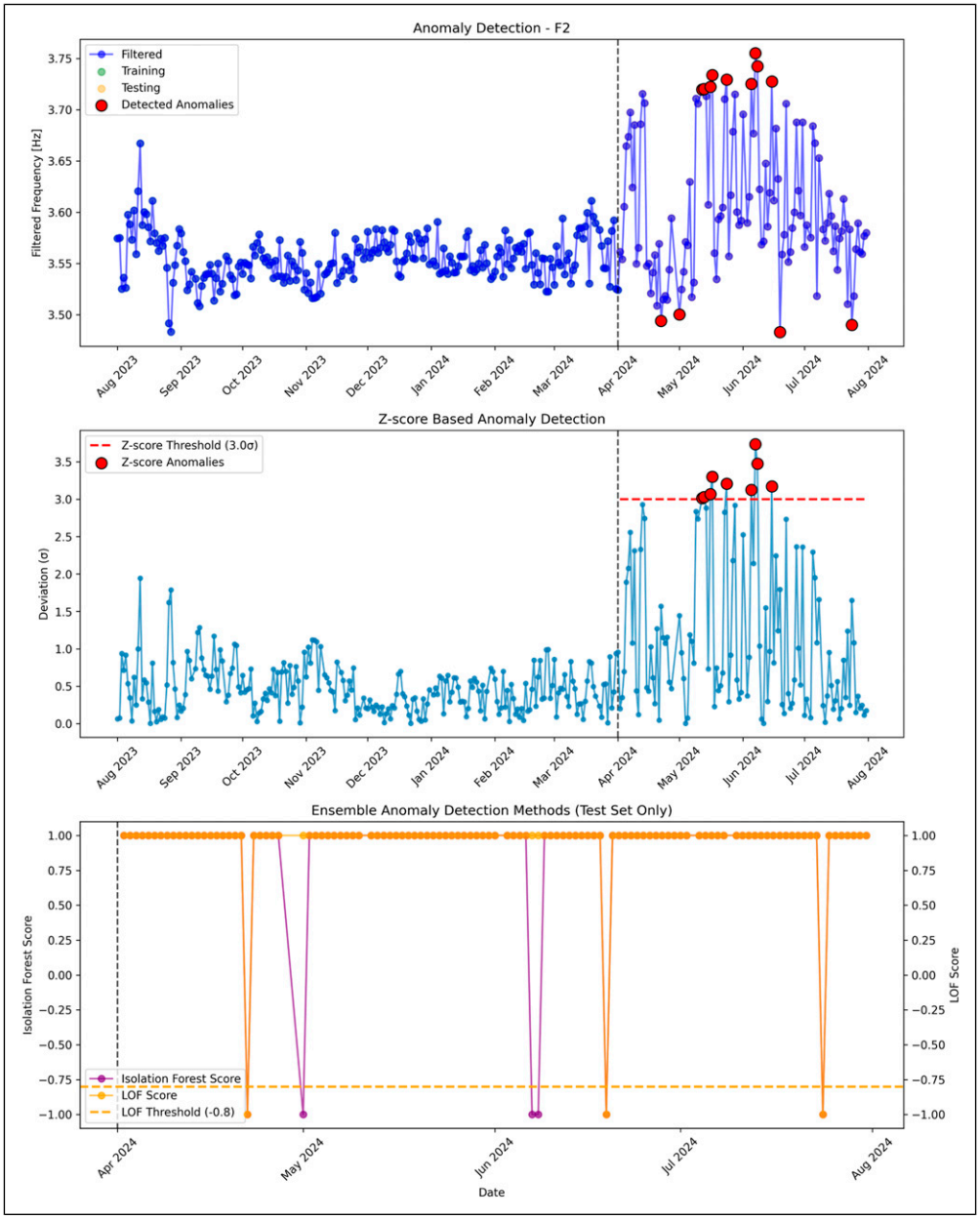

Figure 13. Multi-method anomaly detection results for the second natural frequency (f_2). The temporal clustering of anomalies during late spring and early summer transitions suggests residual environmental coupling beyond univariate temperature effects, potentially attributable to differential thermal dynamics between the steel structure and confining masonry.

Methodological advantages and structural health assessment

The multi-method ensemble approach confers several theoretical and practical advantages:

(i) **Robustness to distributional assumptions**: The combination of parametric (z-score) and non-parametric (IF, LOF) methods reduces dependency on specific distributional forms, enhancing detection reliability across diverse operational conditions.
(ii) **Multi-scale anomaly detection**: Global (z-score, IF) and local (LOF) methods capture anomalies across different spatial and temporal scales, ensuring comprehensive coverage of potential failure modes.
(iii) **Temporal integrity preservation**: Exclusive operation on test data maintains the causal structure of predictive modeling while preventing contamination from training artifacts.

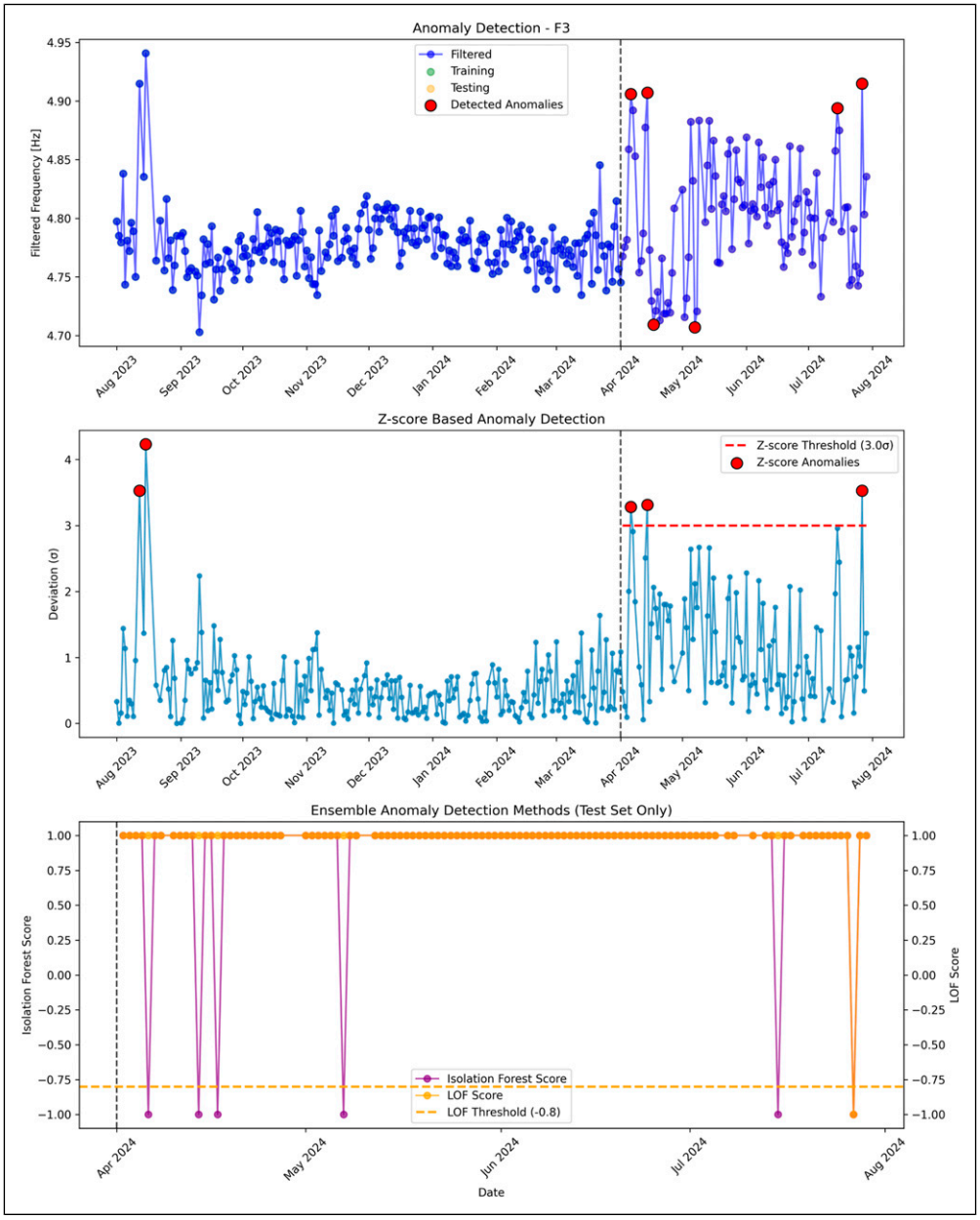

Figure 14. Multi-method anomaly detection results for the third natural frequency (f_3). The torsional mode exhibits the lower anomaly detection rate, demonstrates no persistent patterns indicative of structural degradation, with detected anomalies representing transient deviations rather than systematic deterioration.

The absence of persistent anomaly patterns or progressive frequency shifts throughout the monitoring period supports the conclusion that the Exedra structure maintained stable dynamic properties without evidence of degradation or damage accumulation. The detected anomalies represent transient deviations rather than systematic deterioration, validating both the effectiveness of the temperature compensation methodology and the structural integrity of the monitored system throughout the observation period.

Physical model interpretation

To investigate the variation in modal parameters with temperature, a model updating procedure was performed to analytically represent the experimentally observed behavior of the Exedra structure. The steel-and-glass structure was modeled

in SAP2000 using 3D beam elements for the steel members and zero-mass shell elements for the two horizontal glazed roofs. The shell elements were assigned zero stiffness and used exclusively to apply the equivalent distributed surface load corresponding to the dead weight of the roofs. An elastic and linear constitutive law was adopted for all materials, with Young's modulus $E = 210$ GPa, Poisson's ratio $\nu = 0.3$, and mass density $\rho = 7.849$ kg/m^3 for steel components. The masonry interaction was represented using linear-elastic springs at the interface regions, modeling confinement at the base and lateral supports of the structure. These springs act along translational and (where needed) rotational directions, and are characterized by equivalent stiffness values k_i (e.g., k_x, k_y, k_z, k_{θ_z}), which were calibrated to reproduce the experimentally observed boundary restraint. This reflects the physical situation in which the steel–glass assembly is partially embedded in or braced by the surrounding historic masonry, rather than being free-standing. Each spring stiffness k_i was calibrated through parametric analyses to reproduce the experimentally observed modal frequencies. More details about the FEM model can be found in Ref. [28]. Given that the structure is composed of steel and glass, it was initially expected that increasing temperatures would decrease natural frequencies due to thermal expansion and reduced stiffness. However, experimental monitoring and modal identification revealed a slight increase in frequency at higher temperatures. This unexpected behavior can be attributed to the confining effect of the surrounding old masonry structure. The Exedra is embedded within the historical buildings, with steel brackets penetrating the masonry to secure the structure. As the temperature increases, the confining effect of the masonry structure becomes predominant. This stiffness enhancement due to confinement likely outweighs the expected decrease in stiffness from thermal effects, leading to an increase in natural frequencies up to 6.7% (Table 4).

To account for this behavior, the connection of steel to the historical buildings was adjusted during the model updating process, considering the four modeling strategies summarized in Table 5. In Model 1 and 2, the joints connecting the steel structure to the masonry building have been restrained as clamps and hinges, respectively. In Model 3 and 4, the interaction between the two structures has been modeled through spring constraints. The stiffness of the springs was adjusted to obtain the maximum (Model 3) and minimum (Model 4) values of the experimental natural frequencies (Figure 15) whose mode shapes are plotted in Figure 16. It can be noted that the high spring stiffness values in $x-$ and $y-$ direction (Model 3 in Table 5) return the highest experimental frequencies across the first three modes (Figure 15), while the low spring stiffness values (Model 4) result in the lowest experimental frequencies, without altering the order of the mode shapes (y, x, and r_z directions). The spring stiffness values k_x, k_y, k_z, and k_{r_z} were identified through an iterative trial-and-error calibration process, progressively adjusting the stiffness of the steel–masonry interface to reproduce the experimentally observed natural frequencies for the first three modes. The two resulting configurations correspond to the upper and lower bounds of the experimental frequency range, representing high- and low-restraint conditions of the actual structure. This modification improved the analytical model's ability to capture the experimentally observed frequency increase with rising temperatures. Similar phenomena have been observed in structures where confinement or interaction with surrounding materials alters expected thermal effects. For instance, Pellegrini et al.[35] have investigated the dynamic behavior of brick masonry walls under temperature changes, highlighting how confinement and material interactions influence mechanical properties and modal responses. They demonstrate that boundary conditions can alter overall stiffness under thermal loads. In addition to masonry confinement, the Exedra roof behaves as a hybrid cable–glass–steel shell system supported by spider nodes and local anchorage, rather than as a uniform steel diaphragm. Temperature-induced geometric stiffening of this assembly, for example, re-tensioning of cable paths and redistribution of in-plane action in the glass panels, may also contribute to the observed increase in natural frequencies with temperature. This thermo–geometric coupling is the subject of ongoing high-fidelity modeling work.

Limitations, simplifications, and physics-informed enhancement

The proposed framework relies on a series of simplifying assumptions. The finite-element model was developed under linear-elastic behavior, using uniform thermal loading and an equivalent spring-based boundary representation to simulate

Table 4. Experimental natural frequencies variation.

	Min	Max	Variation
Mode 1: y-dir	2.98	3.17	6.7%
Mode 2: x-dir	3.48	3.70	6.3%
Mode 3: r_z-tors	4.73	4.84	2.3%

Table 5. Model updating strategies.

	Model 1	Model 2	Model 3	Model 4
Joint restraints	Clamps	Hinges	-	-
k_x (kN/m)	-	-	10^3	220
k_y (kN/m)	-	-	6×10^3	2.5×10^3
k_z (kN/m)	-	-	5×10^3	5×10^3
k_{r_z} (kNm/rad)	-	-	10^7	10^7

the masonry confinement. The temperature input was treated as a scalar variable, neglecting spatial gradients. Uncertainty propagation and variance-based sensitivity analyses have not yet been performed. However, the present deterministic framework can be readily extended toward stochastic physics-informed formulations, where variance-based sensitivity indices and probabilistic energy functionals are used to quantify the influence of uncertain input parameters on the modal

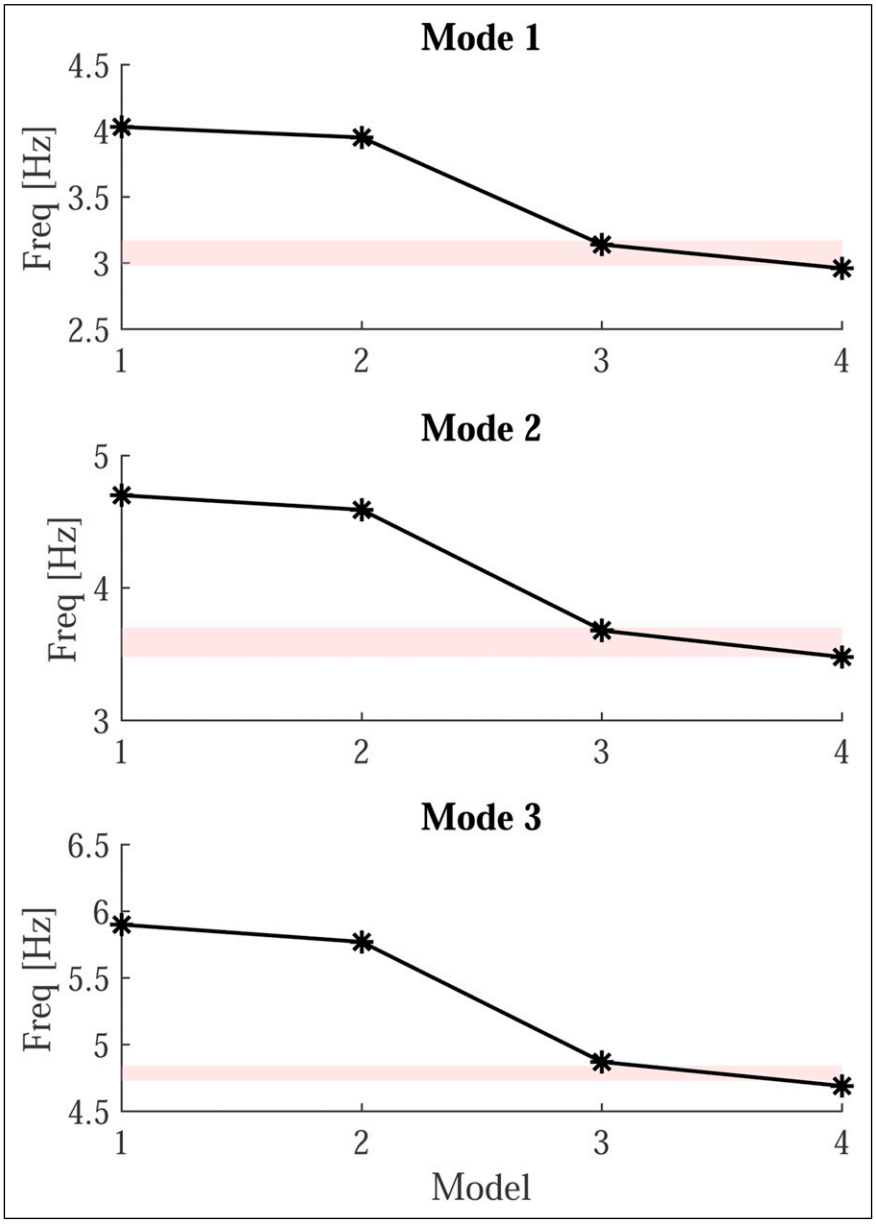

Figure 15. Numerical frequency of the first three modes as a function of the model updating. The shaded bands represent the experimental frequency range (minimum–maximum).

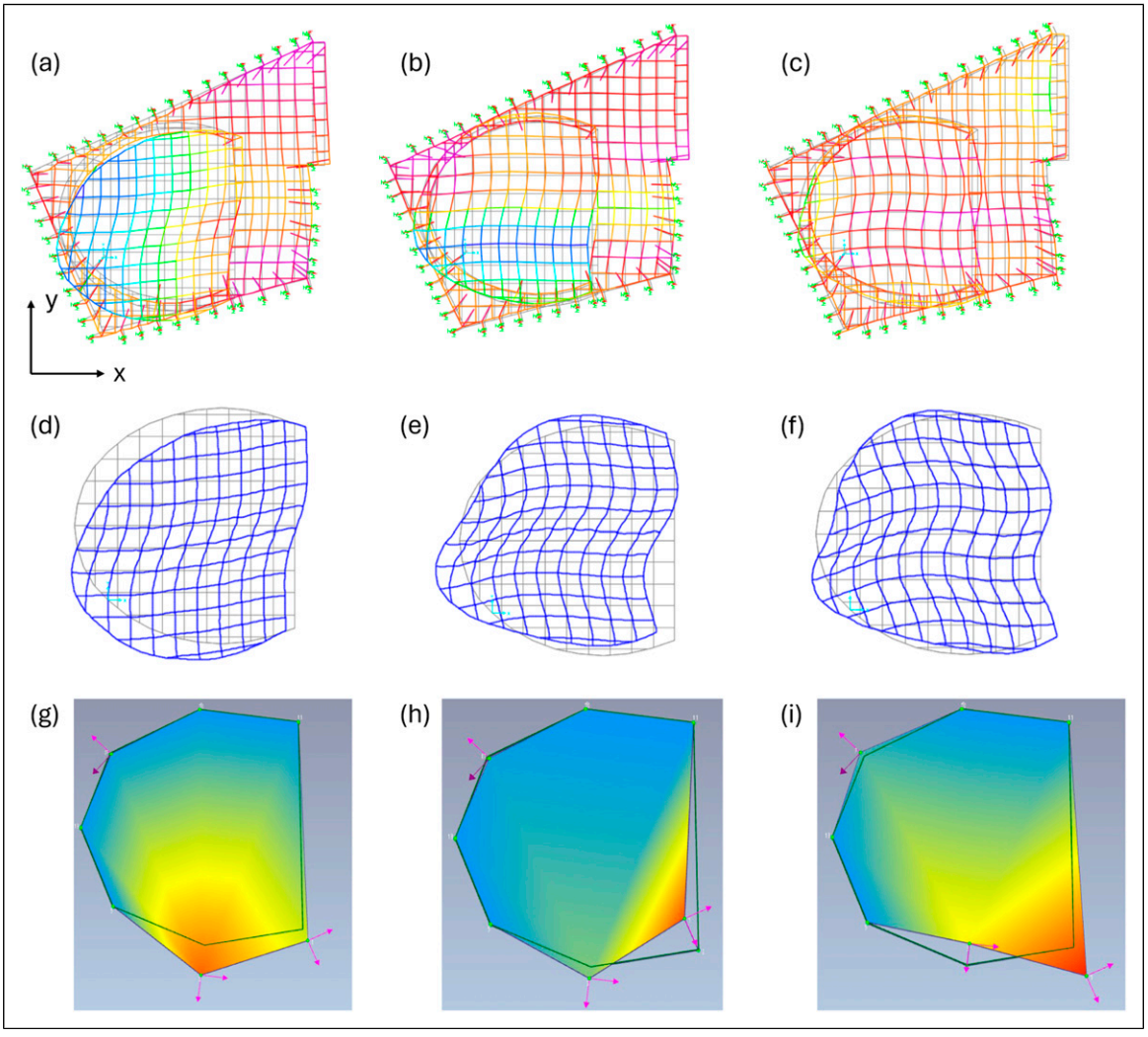

Figure 16. Top view of numerical (global, a-c, and zoomed-in view of the dome, d-f) and experimental (g-i) mode shapes: first mode in the *y*-direction (a, d, g), second mode in the *x*-direction (b, e, h), torsional mode in the r_z-direction (c, f, i).

response. In the current deterministic framework, the interface spring stiffnesses were calibrated through trial-and-error matching with experimental modal data. Future work will explicitly treat these parameters as stochastic variables and propagate their variability to the predicted modal properties using variance-based sensitivity analysis. These simplifications constrain the generality of the approach but ensure interpretability and numerical stability when applied to long-term monitoring data. To improve the physical consistency of the data-driven component, a preliminary physics-informed NN variant was implemented. In addition to the standard mean-square prediction loss, a regularization term was introduced to penalize deviations between the learned temperature–frequency slope ($\partial f_2/\partial T$) and the thermomechanical trend derived from FEM-supported regression. This PINN-like constraint enforces the experimentally observed monotonic increase of frequency with temperature, associated with confinement-induced stiffening of the Exedra's steel–glass frame. The regularization term is analogous to those used in physics-informed neural networks,[36] where physical consistency acts as a stabilizing constraint in learning from sparse or noisy data. Conceptually, this hybrid formulation bridges the proposed ANN-FEM strategy with energy-based and neural-operator frameworks, such as the Deep Energy Method (DEM)[37] and the Variationally Consistent Neural Operator (VINO),[38] which are identified as promising directions for future SHM developments. The comparative performance of the three compensation models (linear regression, purely data-driven ANN, and physics-informed ANN) is summarized in Table 3. The physics-informed (PI) network yields slightly higher RMSE but provides smoother and physically interpretable temperature–frequency trends, confirming its role as a robust regularizer. Although the linear regression provided a reasonable first-order approximation of the temperature–frequency trend, the nonlinear ANN achieved lower residual variance and smoother predictions, particularly near temperature extremes where

the experimental response slightly deviates from linearity. The ANN's ability to capture weak thermomechanical nonlinearities and its compatibility with the physics-informed constraint justify its selection as the main compensation model, while the linear regression remains a useful baseline reference.

The results confirm that the physics-informed formulation maintains comparable numerical accuracy while ensuring physically interpretable and smoother temperature–frequency relationships across all modes. A limitation of the present study is that the environmental temperature data were obtained from the nearby Roma Colosseo meteorological station rather than from on-structure sensors. Although this introduces minor uncertainty associated with local radiative or airflow effects, the proximity and similar exposure of the two sites make this dataset a reliable proxy for the boundary temperature. Future monitoring will integrate on-site temperature sensors to capture micro-climatic gradients directly on the steel–glass frame.

Conclusions and future work

Continuous identification of natural frequencies offers valuable insights into the condition of civil structures. Careful consideration of environmental impacts is essential for accurate evaluations. Integrating temperature compensation methods into vibration-based damage identification systems is crucial for improving accuracy, while neglecting temperature effects can lead to erroneous conclusions about structural health, potentially compromising safety. These findings have significant implications for SHM practices, especially for historic buildings, where safeguarding cultural heritage is paramount. The paper highlights the importance of integrating data-driven advanced identification techniques and model-based approaches in SHM to preserve cultural heritage structures. While the ANN effectively filtered environmental effects, enhancing modal identification accuracy, the model-based analysis provides a valuable tool for accounting for discrepancies between numerical and experimental modal parameters, which are crucial for preservation efforts in historical structures. The established temperature–frequency relationships can be used to compensate for environmental effects in real-time monitoring, enhancing the sensitivity to actual structural changes. The filtered frequencies provide a more reliable baseline for future assessments, with alert thresholds set at $\pm 3\sigma$ from the mean values.

The methodology contributes to the broader field of structural health monitoring by demonstrating effective approaches for filtering environmental effects in complex structures with unique thermal–structural interactions. The integration of neural network-based temperature compensation with multi-method anomaly detection provides a robust framework for distinguishing between environmental variations and genuine structural changes.

The comparative analysis reveals insights into the trade-offs between computational simplicity and physical fidelity in temperature compensation strategies. The deterministic least-squares optimization employed for the compact baseline ANN ensures stable convergence and reproducible results, while the PINN's gradient-based training incorporates early stopping mechanisms to prevent overfitting to the limited training dataset. This distinction becomes particularly relevant when considering the generalization capabilities of each approach. A critical advantage of the physics-informed formulation emerges in its handling of out-of-distribution scenarios, particularly during seasonal transitions where purely data-driven models exhibit degraded performance. By anchoring both the sign and magnitude of temperature sensitivity through the monotonicity and slope constraints, the PINN maintains physically plausible predictions even when encountering temperature ranges sparsely represented in the training data. This robustness is essential for continuous monitoring systems that must operate reliably across full annual cycles with varying environmental conditions.

Furthermore, the interpretability of the physics-informed approach addresses a fundamental concern in structural health monitoring applications. Unlike black-box neural networks, the effective temperature sensitivity can be directly examined through finite-difference approximations of $\partial\widehat{f}/\partial T$, while explicit penalization of monotonicity violations ensures that the learned relationships remain consistent with established thermomechanical principles. This transparency facilitates validation by domain experts and builds confidence in automated damage detection systems.

The observed increase in natural frequencies with temperature in the Exedra structure highlights the importance of considering the interaction between the structure and its surroundings in thermal analyses. The experimentally obtained results suggest that the overall direct relationship between natural frequencies and temperature observed during long-term monitoring is due to confinement phenomena within the surrounding masonry. By preventing expansion, this interaction leads to the closure of micro-cracks and consequent stiffening, despite the well-known negative effect of temperature on the stiffness of steel. This finding is consistent with analogous cases in the literature where confinement effects dominate thermally induced stiffness reductions.

Future work will focus on the long-term validation of these filtering approaches, investigating additional environmental influences beyond temperature, and integrating further parameters such as damping ratios and mode shapes to achieve a

more comprehensive structural diagnosis. The extension of these methodologies to other heritage structures with similar confinement characteristics will enable validation of the observed positive temperature–frequency correlations and further demonstrate the robustness and generalizability of the proposed framework.

Acknowledgments

The authors are gratefully acknowledged to the ©Sovrintendenza Capitolina.

ORCID iD

Marianna Crognale https://orcid.org/0000-0002-2190-1866

Funding

The research project reported in this paper was part of ERIS Project supported by LAZIO INNOVA (n. G09493 - PO FESR LAZIO 2014/2020). The research project reported in this paper was part of IRIS (Inspection and security by Robots interacting with Infrastructure digital twins) Project supported by the NATO Science for Peace and Security Programme (grant SPS.MYP.G5924). EU LIFE-ASTI project "Implementation of a forecasting system for urban heat island effect for the development of urban adaptation strategy" (LIFE17 CCA/GR/000108). LIFE21-GIE-EL-LIFE project "A System for Integrated Environmental Information in Urban Areas (SIRIUS)." Institute of Atmospheric Sciences and Climate (ISAC) of the National Research Council (CNR), Via Fosso del Cavaliere 100, 00133 Rome, Italy. Meteo LazioTM amateur weather network. Website: https://www.meteoregionelazio.it.

Declaration of conflicting interests

The authors declared no potential conflicts of interest with respect to the research, authorship, and/or publication of this article.

Data Availability Statement

The datasets supporting the findings of this study will be made publicly available on Zenodo upon publication.

References

1. Deraemaeker A, Reynders E, De Roeck G, et al. "Vibration-based structural health monitoring using output-only measurements under changing environment". *Mech Syst Signal Process* 2008; 22(1): 34–56.
2. Peeters B and De Roeck G. "Reference-based stochastic subspace identification for output-only modal analysis". *Mech Syst Signal Process* 1999; 13(6): 855–878.
3. Magalhães F and Cunha Á. "Explaining operational modal analysis with data from an arch bridge". *Mech Syst Signal Process* 2011; 25(5): 1431–1450.
4. Rinaldi C, Crognale M, Ciambella J, et al. "Automated operational modal analysis using a large data set from continuous monitoring". In *XXVI AIMETA Congress Italian Association of Theoretical and Applied Mechanics Napoli*, 2025.
5. Xia Y, Chen B, Weng S, et al. Temperature effect on vibration properties of civil structures: a literature review and case studies. *Journal of Civil Structural Health Monitoring* 2012; 2: 29–46.
6. Ubertini F, Comanducci G, Cavalagli N, et al. "Environmental effects on natural frequencies of the San Pietro bell tower in Perugia, Italy, and their removal for structural performance assessment". *Mech Syst Signal Process* 2017; 82: 307–322.
7. Luo J, Huang M and Lei Y. "Temperature effect on vibration properties and vibration-based damage identification of bridge structures: a literature review". *Buildings* 2022; 12: 1209.
8. Kang F, Liu X and Li J. "Temperature effect modeling in structural health monitoring of concrete dams using kernel extreme learning machines". *Struct Health Monit* 2020; 19(4): 987–1002.
9. Bao Y, Xia Y, Li H, et al. "Data fusion-based structural damage detection under varying temperature conditions". *Int J Struct Stabil Dynam* 2012; 12(6): 1250052.
10. Liu W, Yang N, Bai F, et al. "An improved automated framework for operational modal analysis with multi-stage clustering and modal quality evaluation". *Mech Syst Signal Process* 2024; 212: 111235.
11. Rinaldi C, Crognale M, Ciambella J, et al. "Long-Term Vibrational Monitoring of the Exedra of Marcus Aurelius' Hall". In: *International operational modal analysis conference*, 2024, pp. 130–137.
12. Mousavi M and Gandomi AH. "Structural health monitoring under environmental and operational variations using MCD prediction error". *J Sound Vib* 2021; 512: 116370.

13. Zhang D, Bao Y, Li H, et al. "Investigation of temperature effects on modal parameters of the China National Aquatics Center". *Adv Struct Eng* 2012; 15(7): 1139–1153.
14. Regni M, Arezzo D, Carbonari S, et al. "Effect of Environmental Conditions on the Modal Response of a 10-Story Reinforced Concrete Tower". *Shock Vib* 2018; 2018(1): 9476146.
15. Kita A, Cavalagli N and Ubertini F. Temperature effects on static and dynamic behavior of Consoli Palace in Gubbio, Italy. *Mech Syst Signal Process* 2019; 120: 180–202.
16. Jiao Y, Liu H, Wang X, et al. "Temperature effect on mechanical properties and damage identification of concrete structure". *Adv Mater Sci Eng* 2014; 2014(1): 1–10.
17. Meruane V and Heylen W. "Structural damage assessment under varying temperature conditions". *Struct Health Monit* 2012; 11(3): 345–357.
18. Huang M-S, Gül M and Zhu H-P. "Vibration-based structural damage identification under varying temperature effects". *J Aero Eng* 2018; 31(3): 04018014.
19. Huang M-S, Cheng S-X, Zhang H-Y, et al. "Structural damage identification under temperature variations based on PSO–CS hybrid algorithm". *Int J Struct Stabil Dynam* 2019; 19(11): 1950139.
20. Wang Z, Huang M and Gu J. "Temperature effects on vibration-based damage detection of a reinforced concrete slab". *Applied Sciences* 2020; 10(8): 2869.
21. Ding YL and Li AQ. "Temperature-induced variations of measured modal frequencies of steel box girder for a long-span suspension bridge". *International Journal of Steel Structures* 2011; 11: 145–155.
22. Kamali S, Marzani A, Sciullo L, et al. "Temperature compensation in vibration-based structural health monitoring using neural network regression". In: Proceedings of the 7th international conference on System reliability and safety, (ICSRS 2023), Palermo, Italy, 23–25 November 2023, pp. 36–42, IEEE.
23. Zhou HF, Ni YQ and Ko JM. "Performance of neural networks for simulation and prediction of temperature-induced modal variability," *Smart Structures and Materials 2005: Sensors and Smart Structures Technologies for Civil, Mechanical, and Aerospace Systems, SPIE Proceedings*, Vol. 5765, San Diego, CA, USA, 7–10 March 2005, pp. 912–922.
24. Gu J, Gul M and Wu X. "Damage detection under varying temperature using artificial neural networks". *Struct Control Health Monit* 2017; 24(11): e1998.
25. Markou M and Singh S. "Novelty detection: a review—part 2: neural network based approaches". *Signal Process* 2003; 83(12): 2499–2521.
26. Narasimhan S. "Robust direct adaptive controller for the nonlinear highway bridge benchmark". *Struct Control Health Monit: The Official Journal of the International Association for Structural Control and Monitoring and of the European Association for the Control of Structures* 2009; 16(6): 599–612.
27. Suresh S, Narasimhan S, Nagarajaiah S, et al. "Fault-tolerant adaptive control of nonlinear base-isolated buildings using EMRAN". *Eng Struct* 2010; 32(8): 2477–2487.
28. Crognale M, Rinaldi C, Potenza F, et al. "Developing and testing high-performance SHM Sensors Mounting Low-Noise MEMS accelerometers". *Sensors* 2024; 24(8): 2435.
29. Luo W, Chen W, Liu D, et al. "Effect of temperature and humidity on mechanical properties and constitutive modeling of pressure-sensitive adhesives". *Sci Rep* 2024; 14(1): 14634.
30. Li X, Cai X, Li S, et al. "Analysis of the structural behavior evolution of reinforced soil retaining walls under the combined effects of rainfall and earthquake". *Buildings* 2024; 15(1): 115.
31. Goodfellow I, Bengio Y and Courville A. *Deep learning*. MIT press, 2016.
32. Haykin SS. *Neural networks and learning machines*. Pearson Education, 2009.
33. CEN. *"Eurocode 3: design of steel structures – part 1-2: structural fire design", EN 1993-1-2*. European Committee for Standardization, 2005.
34. Rodgers JL and Nicewander WA. "Thirteen ways to look at the correlation coefficient". *Am Statistician* 1988; 42(1): 59–66.
35. Pellegrini D, Barontini A, Mendes N, et al. Dynamic response of masonry structures to temperature variations: experimental investigation of a brick masonry Wall. *Sensors* 2024; 24(23): 7573.
36. Raissi M, Perdikaris P and Karniadakis GE. "Physics-informed neural networks: a deep learning framework for solving forward and inverse problems involving nonlinear partial differential equations". *J Comput Phys* 2019; 378: 686–707.
37. Samaniego E, Anitescu C, Goswami S, et al. "An energy approach to the solution of partial differential equations in computational mechanics via machine learning: concepts, implementation and applications". *Comput Methods Appl Mech Eng* 2020; 362: 112790.
38. Eshaghi MS, Anitescu C, Thombre M, et al. "Variational Physics-informed Neural Operator (VINO) for solving partial differential equations". *Comput Methods Appl Mech Eng* 2025; 437: 117785.